Generation of Bright, Spatially Coherent Soft X-Ray High Harmonics in a Hollow Waveguide Using Two-Color Synthesized Laser Pulses

Cheng Jin,[1,*] Gregory J. Stein,[2] Kyung-Han Hong,[2] and C. D. Lin[1]
[1]*J. R. Macdonald Laboratory, Department of Physics, Kansas State University, Manhattan, Kansas 66506, USA*
[2]*Department of Electrical Engineering and Computer Science and Research Laboratory of Electronics, Massachusetts Institute of Technology (MIT), Cambridge, Massachusetts 02139, USA*
(Received 17 February 2015; published 22 July 2015)

We investigate the efficient generation of low-divergence high-order harmonics driven by waveform-optimized laser pulses in a gas-filled hollow waveguide. The drive waveform is obtained by synthesizing two-color laser pulses, optimized such that highest harmonic yields are emitted from each atom. Optimization of the gas pressure and waveguide configuration has enabled us to produce bright and spatially coherent harmonics extending from the extreme ultraviolet to soft x rays. Our study on the interplay among waveguide mode, atomic dispersion, and plasma effect uncovers how dynamic phase matching is accomplished and how an optimized waveform is maintained when optimal waveguide parameters (radius and length) and gas pressure are identified. Our analysis should help laboratory development in the generation of high-flux bright coherent soft x rays as tabletop light sources for applications.

DOI: 10.1103/PhysRevLett.115.043901 PACS numbers: 42.65.Ky, 31.70.Hq, 33.80.Rv

In science and technology, light sources in different specific spectral regions are often needed for numerous applications, such as photochemistry, imaging, and material processing. Large national facilities like synchrotron radiation sources or free-electron lasers have been built to serve these purposes. However, it is desirable that broadband lights are available as dedicated tabletop equipment in more laboratories. From nonlinear optics, it has been known that laser light can be converted from one wavelength to another. Recent research has shown that the extreme nonlinear interaction of infrared lasers with gas media can generate high-order harmonics (HHs) extending to 1.5 keV [1]. Today, the main limitation that prevents HH from evolving as a useful light source is its low conversion efficiency.

To improve harmonic efficiency, multicolor sinusoidal fields have been synthesized to modify the drive waveform in a way such that harmonic emission from each atom can be enhanced [2–9]. This approach has become very favorable recently because of technological advances in optics [10–19]. In our recent works [8,9], a general optimization scheme was proposed to obtain the best waveform such that the maximum HH yield from a single atom can be achieved by synthesizing two- or three-color fields. The harmonics generated from such an optimized waveform are better phase matched in the gas medium; thus, they would also exhibit better spatial coherence. These harmonics are important for applications, especially for coherent x-ray imaging, since refocusing beams in these spectral ranges incurs large energy loss.

In this Letter, we choose a hollow waveguide filled with gas as the generating medium because the diffraction of the laser beam is eliminated and nearly constant laser intensity can be maintained for an extended interaction length, which are favorable to the phase matching in general. The waveguide further decouples the laser's geometric phase along the radial distance. This makes the hollow waveguide an ideal setup to keep a constant waveform as the laser propagates. The hollow waveguide has been widely used [20] in harmonic generation experiments: for temporal and spatial pulse shaping of the driving laser [21,22], quasiphase matching (QPM) [23,24], fully phase-matched harmonic generation [25–27], cutoff extension with mid-infrared lasers [28,29], and the selection of electron trajectories [30].

To achieve highly efficient, bright HH generation in the soft x-ray range, we propose to combine two advanced laser technologies: waveform synthesis and laser guiding by the waveguide. We identify the optimal conditions for generating best-quality harmonics and uncover the underlying mechanism of dynamic phase matching. We show that the best phase-matched harmonics from the extreme ultraviolet (XUV) to soft x rays have low divergences (smaller than 1 mrad), which can be compared to vacuum ultraviolet (VUV) or XUV harmonics generated by traditional 800-nm lasers [31–36]. In comparison, soft x-ray harmonics generated with a midinfrared laser alone reported the full divergence angle of about 7 mrad [37] or 4 to 8 mrad [38] (half divergence angle should be compared to 1 mrad). The details of our simulations are given in the Supplemental Material [39].

To discuss the benefit of using a synthesized waveform, we first show the total harmonic yield at the exit of the hollow waveguide (near field) generated by the waveform (WF) of 1.6- and 0.533-μm laser pulses in Fig. 1(a). The laser parameters are shown in Table I (see WF1). To achieve the highest cutoff of about 250 eV (close to the single-atom cutoff) and the highest harmonic yield

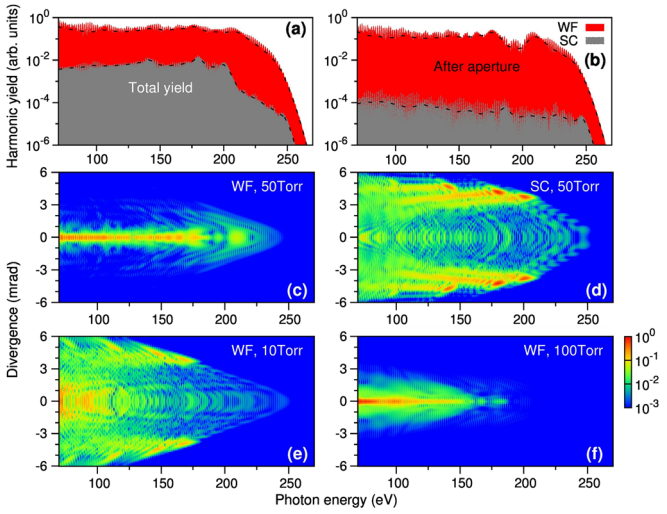

FIG. 1 (color online). (a) Total harmonic yield emitted at the exit of the hollow waveguide and (b) harmonic yield integrated within 1 mrad using an aperture in the far field for two-color ($1.6 + 0.533\ \mu$m) waveform (WF1 in Table I) and single-color (SC) laser, where gas pressure is 50 torr. The corresponding harmonic divergences in the far field given for WF1 (c) and for SC (d). Harmonic divergences of WF1 shown for two other gas pressures: 10 torr (e) and 100 torr (f). Length and radius of the waveguide are 5 mm and 125 μm, respectively. The vertical fringes in (c)–(f) represent individual harmonics.

simultaneously, we have varied both the waveguide length and the gas pressure, and found that the optimal values were 5 mm and 50 torr. In Fig. 1(a), we also show the total harmonic yield generated by the 1.6-μm laser alone with the peak intensity of 3.0×10^{14} W/cm^2 under the same condition. Clearly, WF1 generates harmonic yields about 1 to 2 orders of magnitude higher than the single-color (SC) pulse without much increase of the laser power.

The harmonic emissions in the far field for the two cases are shown in Figs. 1(c) and 1(d), where harmonic yields have been normalized to the maximum value in each figure independently. We can see desirable features in harmonics generated with WF1. Figure 1(c) shows that high harmonics covering from 70 to 250 eV are strongly localized at the propagation axis—their divergence is found to be within 1 mrad. For SC [see Fig. 1(d)], the harmonics generated in the same spectral region are located mostly off the axis. If one uses an aperture to filter out harmonics with divergence larger than 1 mrad (this is a common procedure for selecting the generated XUV harmonics as a light source, for example, in attosecond experiments), the harmonic yields with WF1 are mostly unchanged but are reduced significantly with SC. Figure 1(b) shows more than 3 orders of magnitude difference in useful high harmonics when one compares WF1 with SC. Note that the harmonics generated by the optimized waveform (WF1) in free space show poor spatial coherence and reduced plateau (see the Supplemental Material [39]).

We have checked that at the optimal pressure of 50 torr, the spatially coherent, low-divergence high harmonics can still be obtained with the WF1 pulse when the waveguide length is reduced to 3 mm. What about the harmonics if the gas pressure is changed? We consider two pressures, 10 and 100 torr, at the same waveguide length of 5 mm. The results of harmonic emission in the far field are shown in Figs. 1(e) and 1(f). For the 10-torr case, high harmonics are located both on axis and off axis, showing poor spatial distribution even though the cutoff of 250 eV is maintained. For the 100-torr case, the harmonics from 70 to 180 eV have low divergence angles, but the cutoff energy is greatly reduced. These results imply that phase matching of harmonic generation in the gas medium is very complicated. It is of interest to take a closer look at how phase matching works in the three gas pressures studied here.

It is well known that HHs are emitted from the recombination of "long"- and "short"-trajectory electrons with atomic ions. Since the accumulated phase of the long-trajectory harmonics is large and highly dependent on the driving laser intensity, these harmonics not only are difficult to phase match (longitudinal intensity change) but also have a large divergence in the far field (transverse intensity distribution) [57,58]. Therefore, short-trajectory components are favorable for the phase matching of HHs and thereby the generation of bright, low-divergence harmonics with excellent spatial coherence. However, for SC pulses, harmonic yields from each atom are much stronger for the long-trajectory electrons, especially for long-wavelength driving lasers [59]. On the other hand, the optimized waveforms in Ref. [8], including WF1 used here, were obtained to enhance the emission from short-trajectory electrons while suppressing the emission from long-trajectory electrons. Excellent phase matching with a waveform-optimized pulse like WF1 can be achieved when the following two conditions are satisfied: (i) the optimized waveform, especially the optimal relative phase between the two colors, needs to be maintained in the whole interaction volume; and (ii) HHs generated in the medium have to be phase matched over the entire interaction region. In the following, we demonstrate how gas pressure affects dynamic phase matching by evaluating how these two conditions are satisfied inside the waveguide.

As the laser propagates inside the waveguide, it is dispersed by the waveguide mode, neutral atom dispersion, and plasma. These factors enter in the refractive index for each color represented by [22]

$$n_l \approx 1 - \frac{\mu_1^2 \lambda_l^2}{8\pi^2 a^2} + p(1-\eta)\delta_1(\lambda_l) - \frac{p\eta n_0 r_e \lambda_l^2}{2\pi}. \quad (1)$$

Here, μ_1 is the mode factor ($= 2.405$ for fundamental EH_{11} mode), a the radius of the waveguide, p the pressure, η the ionization level, δ_l the neutral atom dispersion, n_0 the neutral atomic density, and r_e the classical electron radius. Each correction term on the right-hand side of Eq. (1) contributes to the time shift (or group delay) with respect to the reference frame (moving at the speed of light). For

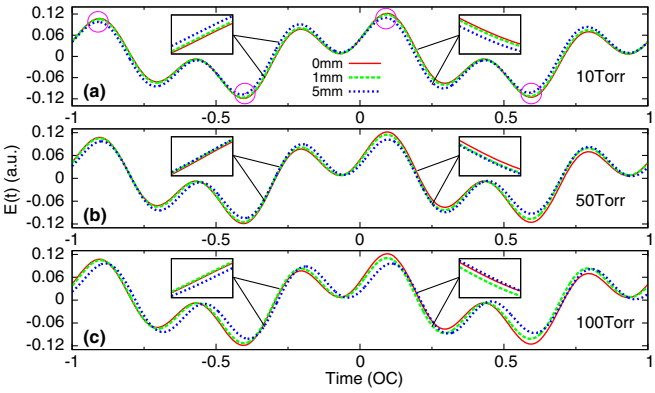

FIG. 2 (color online). On-axis electric fields of two-color waveform at three gas pressures: (a) 10 torr, (b) 50 torr, and (c) 100 torr. The electric fields are shown at the entrance (0 mm), inside (1 mm), and at the exit (5 mm) of the waveguide. Enlarged views of the electric fields are indicated. Circles indicate where the electrons are ionized. Radius of the waveguide is 125 μm (OC means the optical cycle of the 1.6-μm laser).

an ideal full phase-matching condition, the electric field remains the same within the waveguide. However, this is not possible since, due to dispersion, the ionization level decreases with the propagation distance. On the other hand, the ionization level increases with time as the field strength increases. Thus one has to consider dynamic phase-matching conditions.

In Fig. 2, we show the on-axis electric fields in the reference frame at three propagation positions $z = 0$, 1, and 5 mm, for the three gas pressures studied in Fig. 1. For the 10-torr case, we draw attention to electric fields (marked by circles) where electrons are born that are to contribute to the harmonic generation. The phase of the electric field shifts monotonically to the left with increasing z. This leads to phase mismatch between harmonics generated from different positions of the waveguide, thus, resulting in harmonic spectra shown in Fig. 1(e). For the optimal phase-matched pressure of 50 torr, at the same marked times, the electric fields at $z = 1$ and 5 mm (as well as the region in between) overlap very well, indicating the harmonics will be well phase matched. At the leading edge, dispersion from the waveguide mode is compensated by the neutral atom dispersion. At the trailing edge, the atomic dispersion is compensated by the plasma effect. The different behaviors in leading and trailing edges at each z show the dynamic phase-matching features when the laser pulse propagates from the entrance to the exit of the waveguide. If the pressure is increased to 100 torr, the peak electric fields are reduced, leading to significant reduction in cutoff energy. At higher pressure, harmonics from long-trajectory electrons tend to suffer phase mismatch more significantly; thus, large divergence harmonics are not visible anymore [see Fig. 1(f)]. Figure 2 serves to illustrate the effect of pressure on dynamic phase-matching phenomena.

TABLE I. Laser parameters for two-color waveforms. Waveform WF1 is the on-axis initial electric field from Ref. [8]. WF2 mimics the on-axis electric field at the exit of the waveguide (5-mm long and 125-μm radius) filled with neon gas (50 torr). $\lambda_1 = 1600$ nm, $\lambda_2 = \lambda_1/3$, and $\phi_1 = 0$. Peak intensities ($|E_1|^2$ and $|E_2|^2$) are in 10^{14} W/cm^2.

Waveform	$\lvert E_1\rvert^2$	$\lvert E_2\rvert^2$	ϕ_2
WF1	1.98	1.32	1.36 π
WF2	1.80	1.20	1.16 π

We next investigate if the propagated laser pulses maintain their optimized waveforms, especially the relative phases between the two colors. As shown previously in Ref. [8], if the relative phase of a waveform is within $\pm 0.2\pi$ from the optimized value, the short-trajectory harmonics still dominate and the harmonic cutoff and yield can be maintained (see supplementary Fig. 3 for Ref. [8]). For the input WF1, we use WF2 to mimic the on-axis electric field at 5 mm. The parameters of both waveforms are given in Table I and the electric fields are plotted in Fig. 3(a). (Time-frequency analysis of harmonic emission is given in the Supplemental Material [39].) Compared to WF1, the relative phase between the two colors is reduced by 0.2π (equivalent to a time shift of 178 as for the 0.533-μm laser) and the field strength of each color decreases somewhat due to the dispersion effect in the medium.

First, we consider the time shift of each component of the incident two-color pulse due to mode dispersion. In Eq. (1), this term does not depend on the pressure; thus, it is the dominant dispersion term at low pressure. In Table II, the time shift from this term at 5 mm is 200 as for the 1.60-μm component and 22 as for the 0.533-μm component. This accounts for the 178 as time shift in the relative phase compared to WF1. We fix WF1 in the reference frame and move WF2 in Fig. 3(a) 200 as to the left. The resulting field is compared to the electric field calculated from the numerical simulation for the case of 10-torr pressure [see Fig. 3(b)]. Clearly, the two fields overlap well, demonstrating that at low pressure the field inside the waveguide is dominated by the mode dispersion. Next, we consider the time shift at $z = 5$ mm for pressure at 50 torr. Table II shows that the time shifts due to neutral atom dispersion are

TABLE II. Time shift of the two colors with respect to the reference frame at the exit of the waveguide (5-mm long and 125-μm radius) filled with neon gas (50 torr). The ionization level is 0.54%, calculated by the Ammosov-Delone-Krainov (ADK) formula [60,61] at the end of WF2 pulse in Table I. Positive (negative) time means the laser pulse moves faster (slower) than the reference frame.

λ_l	Mode	Atomic	Plasma
1600 nm	200 as	−72.9 as	183 as
533 nm	22 as	−73.4 as	20 as

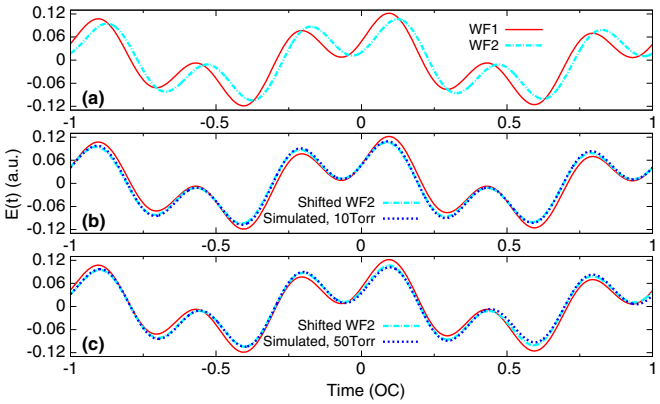

FIG. 3 (color online). (a) Two waveforms from Table I in the reference frame. (b) WF2 in (a) shifted by 200 as to the left. (c) WF2 in (b) shifted by 73 as to the right first, and then shifted to the left by a time-dependent factor $50\eta'(t')$ as. WF1 is the on-axis electric field at the entrance of the waveguide. The electric fields obtained by shifting WF2 are given by dash-dotted lines. In comparison, the electric fields at 5 mm obtained by numerically solving Maxwell's wave equation are shown in dotted lines, for 10 torr and 50 torr in (b) and (c), respectively (OC stands for the optical cycle of the 1.6-μm laser).

about the same for the two colors. If we assume that the ionization level at $z = 5$ mm is constant at 0.54%, the time shifts for the two colors are 183 and 22 as. However, the ionization level also increases with time. The time shift of the laser pulse from the plasma dispersion is time dependent, characterized by a time-dependent factor $50\eta'(t')$ as, where $\eta'(t')$ is the scaled ionization probability. To account for neutral atom dispersion, we move WF2 in Fig. 3(b) by 73 as to the right. Finally, we move it by $50\eta'(t')$ as to the left for the plasma effect. Thus, we obtain the final electric field which is shown to agree well with the numerical one directly from simulation [see Fig. 3(c)]. This analysis demonstrates the different roles played by the three dispersion terms in the waveguide. More details about the calculation of time shift and $\eta'(t')$ are given in the Supplemental Material [39].

In short, we have uncovered that at the optimal condition, the propagated two-color waveforms maintain the same properties as the initial one. Together with dynamic phase matching, highly spatially coherent HHs are thus generated. Note that phase matching only occurs within the central part of a laser pulse at high gas pressure and low ionization level [28,62].

In the discussions above, the radius of the waveguide is fixed at 125 μm. Next, we consider the effect of the waveguide radius, which is another key parameter of a hollow waveguide. We chose two radii, 75 and 200 μm, and searched the optimal waveguide length and gas pressure to ensure the best cutoff and harmonic yield. For 75 (200) μm, the optimal values of length and pressure are 1 mm and 120 torr (7 mm and 20 torr). The incident two-color beam

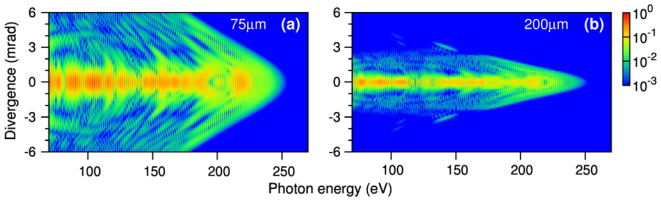

FIG. 4 (color online). Harmonic divergence in the far field for two radii of the waveguide: (a) 75 μm and (b) 200 μm. Gas pressure and length of the waveguide are 120 torr, 1 mm and 20 torr, 7 mm in (a) and (b), respectively. Two-color ($1.6 + 0.533$ μm) synthesized waveform is applied here.

waist is adjusted to ensure that the EH_{11} mode is guided. Thus, the input laser pulse energies are different in these two cases. The normalized harmonic emissions in the far field for two radii are shown in Fig. 4. For both cases, we can see highly localized on-axis harmonic emission. Note that the total harmonic yield of the 200-μm case is much stronger than the 75-μm one (not shown). Therefore, the physical mechanism proposed before is still valid if the radius of the waveguide is changed.

In summary, we investigated the generation of bright and spatially coherent high harmonics from the XUV to soft x rays by using waveform-optimized two-color pulses in a hollow waveguide. The physics behind this behavior is the dynamic phase-matching conditions. With technology advances of the waveform synthesis [16–19,63] and hundreds kHz and MHz high-repetition-rate lasers [34,36,64], our analysis promises to be a powerful tool for realizing all-purpose tabletop coherent light pulses available in many laboratories.

This work was supported by AFOSR FA9550-14-1-0255 and in part by Chemical Sciences, Geosciences, and Biosciences Division, Office of Basic Energy Sciences, Office of Science, U.S. Department of Energy. C. J. thanks Dr. Chien-Jen Lai from MIT for discussing the computational details, and Dr. He Wang and Dr. Wei Cao from Lawrence Berkeley National Laboratory for communication of the experimental status.

*Present address: School of Science, Nanjing University of Science and Technology, Nanjing, Jiangsu 210094, People's Republic of China.

[1] T. Popmintchev *et al.*, Bright coherent ultrahigh harmonics in the keV x-ray regime from mid-infrared femtosecond lasers, Science **336**, 1287 (2012).

[2] S. Watanabe, K. Kondo, Y. Nabekawa, A. Sagisaka, and Y. Kobayashi, Two-Color Phase Control in Tunneling Ionization and Harmonic Generation by a Strong Laser Field and Its Third Harmonic, Phys. Rev. Lett. **73**, 2692 (1994).

[3] I. J. Kim, C. M. Kim, H. T. Kim, G. H. Lee, Y. S. Lee, J. Y. Park, D. J. Cho, and C. H. Nam, Highly Efficient High-Harmonic Generation in an Orthogonally Polarized Two-Color Laser Field, Phys. Rev. Lett. **94**, 243901 (2005).

[4] N. Ishii, A. Kosuge, T. Hayashi, T. Kanai, J. Itatani, S. Adachi, and S. Watanabe, Quantum path selection in high-harmonic generation by a phase-locked two-color field, Opt. Express **16**, 20876 (2008).
[5] L. E. Chipperfield, J. S. Robinson, J. W. G. Tisch, and J. P. Marangos, Ideal Waveform to Generate the Maximum Possible Electron Recollision Energy for Any Given Oscillation Period, Phys. Rev. Lett. **102**, 063003 (2009).
[6] F. Brizuela, C. M. Heyl, P. Rudawski, D. Kroon, L. Rading, J. M. Dahlström, J. Mauritsson, P. Johnsson, C. L. Arnold, and A. L'Huillier, Efficient high-order harmonic generation boosted by below-threshold harmonics, Sci. Rep. **3**, 1410 (2013).
[7] P. Wei, J. Miao, Z. Zeng, C. Li, X. Ge, R. Li, and Z. Xu, Selective Enhancement of a Single Harmonic Emission in a Driving Laser Field with Subcycle Waveform Control, Phys. Rev. Lett. **110**, 233903 (2013).
[8] C. Jin, G. Wang, H. Wei, A. T. Le, and C. D. Lin, Waveforms for optimal sub-keV high-order harmonics with synthesized two- or three-colour laser fields, Nat. Commun. **5**, 4003 (2014).
[9] C. Jin, G. Wang, A. T. Le, and C. D. Lin, Route to optimal generation of soft x-ray high harmonics with synthesized two-color laser pulses, Sci. Rep. **4**, 7067 (2014).
[10] B. E. Schmidt *et al.*, Frequency domain optical parametric amplification, Nat. Commun. **5**, 3643 (2014).
[11] K.-H. Hong, C.-J. Lai, J. Siqueira, P. Krogen, J. Moses, C.-L. Chang, G. J. Stein, L. E. Zapata, and F. X. Kärtner, Multi-mJ, kHz, 2.1 μm optical parametric chirped-pulse amplifier and high-flux soft x-ray high-harmonic generation, Opt. Lett. **39**, 3145 (2014).
[12] C. Vozzi, F. Calegari, F. Frassetto, L. Poletto, G. Sansone, P. Villoresi, M. Nisoli, S. De Silvestri, and S. Stagira, Coherent continuum generation above 100 eV driven by an ir parametric source in a two-color scheme, Phys. Rev. A **79**, 033842 (2009).
[13] H.-C. Bandulet, D. Comtois, E. Bisson, A. Fleischer, H. Pépin, J.-C. Kieffer, P. B. Corkum, and D. M. Villeneuve, Gating attosecond pulse train generation using multicolor laser fields, Phys. Rev. A **81**, 013803 (2010).
[14] T. Siegel *et al.*, High harmonic emission from a superposition of multiple unrelated frequency fields, Opt. Express **18**, 6853 (2010).
[15] E. J. Takahashi, P. Lan, O. D. Mücke, Y. Nabekawa, and K. Midorikawa, Infrared Two-Color Multicycle Laser Field Synthesis for Generating an Intense Attosecond Pulse, Phys. Rev. Lett. **104**, 233901 (2010).
[16] S.-W. Huang *et al.*, High-energy pulse synthesis with sub-cycle waveform control for strong-field physics, Nat. Photonics **5**, 475 (2011).
[17] A. Wirth *et al.*, Synthesized light transients, Science **334**, 195 (2011).
[18] E. J. Takahashi, P. Lan, O. D. Mücke, Y. Nabekawa, and K. Midorikawa, Attosecond nonlinear optics using gigawatt-scale isolated attosecond pulses, Nat. Commun. **4**, 2691 (2013).
[19] S. Haessler *et al.*, Optimization of Quantum Trajectories Driven by Strong-Field Waveforms, Phys. Rev. X **4**, 021028 (2014).
[20] E. Constant, D. Garzella, P. Breger, M. Mével, Ch. Dorrer, C. Le Blanc, F. Salin, and P. Agostini, Optimizing High Harmonic Generation in Absorbing Gases: Model and Experiment, Phys. Rev. Lett. **82**, 1668 (1999).
[21] R. Bartels, S. Backus, E. Zeek, L. Misoguti, G. Vdovin, I. P. Christov, and M. M. Murnane, Shaped-pulse optimization of coherent emission of high-harmonic soft x-rays, Nature (London) **406**, 164 (2000).
[22] C. Winterfeldt, C. Spielmann, and G. Gerber, Colloquium: Optimal control of high-harmonic generation, Rev. Mod. Phys. **80**, 117 (2008).
[23] E. A. Gibson *et al.*, Coherent soft x-ray generation in the water window with quasi-phase matching, Science **302**, 95 (2003).
[24] X. Zhang, A. L. Lytle, T. Popmintchev, X. Zhou, H. C. Kapteyn, M. M. Murnane, and O. Cohen, Quasi-phase-matching and quantum-path control of high-harmonic generation using counterpropagating light, Nat. Phys. **3**, 270 (2007).
[25] A. Rundquist, C. G. Durfee III, Z. Chang, C. Herne, S. Backus, M. M. Murnane, and H. C. Kapteyn, Phase-matched generation of coherent soft x-rays, Science **280**, 1412 (1998).
[26] C. G. Durfee III, A. R. Rundquist, S. Backus, C. Herne, M. M. Murnane, and H. C. Kapteyn, Phase Matching of High-Order Harmonics in Hollow Waveguides, Phys. Rev. Lett. **83**, 2187 (1999).
[27] F. Ardana-Lamas, G. Lambert, A. Trisorio, B. Vodungbo, V. Malka, P. Zeitoun, and C. P. Hauri, Spectral characterization of fully phase-matched high harmonics generated in a hollow waveguide for free-electron laser seeding, New J. Phys. **15**, 073040 (2013).
[28] T. Popmintchev, M.-C. Chen, A. Bahabad, M. Gerrity, P. Sidorenko, O. Cohen, I. P. Christov, M. M. Murnane, and H. C. Kapteyn, Phase matching of high harmonic generation in the soft and hard x-ray regions of the spectrum, Proc. Natl. Acad. Sci. U.S.A. **106**, 10516 (2009).
[29] M.-C. Chen, P. Arpin, T. Popmintchev, M. Gerrity, B. Zhang, M. Seaberg, D. Popmintchev, M. M. Murnane, and H. C. Kapteyn, Bright, Coherent, Ultrafast Soft X-Ray Harmonics Spanning the Water Window from a Tabletop Light Source, Phys. Rev. Lett. **105**, 173901 (2010).
[30] H. Igarashi, A. Makida, and T. Sekikawa, Electron trajectory selection for high harmonic generation inside a short hollow fiber, Opt. Express **21**, 20632 (2013).
[31] M. Chini, X. Wang, Y. Cheng, H. Wang, Y. Wu, E. Cunningham, P.-C. Li, J. Heslar, D. A. Telnov, S.-I Chu, and Z. Chang, Coherent phase-matched VUV generation by field-controlled bound states, Nat. Photonics **8**, 437 (2014).
[32] D. G. Lee, H. T. Kim, K. H. Hong, C. H. Nam, I. W. Choi, A. Bartnik, and H. Fiedorowicz, Generation of bright low-divergence high-order harmonics in a long gas jet, Appl. Phys. Lett. **81**, 3726 (2002).
[33] X. He, M. Miranda, J. Schwenke, O. Guilbaud, T. Ruchon, C. Heyl, E. Georgadiou, R. Rakowski, A. Persson, M. B. Gaarde, and A. L'Huillier, Spatial and spectral properties of the high-order harmonic emission in argon for seeding applications, Phys. Rev. A **79**, 063829 (2009).
[34] I. Pupeza *et al.*, Compact high-repetition-rate source of coherent 100 eV radiation, Nat. Photonics **7**, 608 (2013).

[35] A. Dubrouil, O. Hort, F. Catoire, D. Descamps, S. Petit, E. Mével, V. V. Strelkov, and E. Constant, Spatiospectral structures in high-order harmonic beams generated with terawatt 10-fs pulses, Nat. Commun. **5**, 4637 (2014).

[36] S. Hädrich, A. Klenke, J. Rothhardt, M. Krebs, A. Hoffmann, O. Pronin, V. Pervak, J. Limpert, and A. Tünnermann, High photon flux table-top coherent extreme-ultraviolet source, Nat. Photonics **8**, 779 (2014).

[37] E. J. Takahashi, T. Kanai, K. L. Ishikawa, Y. Nabekawa, and K. Midorikawa, Coherent Water Window X Ray by Phase-Matched High-Order Harmonic Generation in Neutral Media, Phys. Rev. Lett. **101**, 253901 (2008).

[38] J. Yao, H. Xiong, H. Xu, Y. X. Fu, B. Zeng, W. Chu, Y. Cheng, Z. Z. Xu, X. J. Liu, and J. Chen, A systematic investigation of high harmonic generation using mid-infrared driving laser pulses, Sci. China Phys. Mech. Astron. **53**, 1054 (2010).

[39] See Supplemental Material http://link.aps.org/supplemental/10.1103/PhysRevLett.115.043901, which includes Refs. [40–56], for more detailed descriptions of solving Maxwell's wave equations in a hollow waveguide, high harmonics in the free space, time-frequency analysis of single-atom harmonic emission, and calculating the time shift of laser pulse caused by individual dispersion terms.

[40] M. B. Gaarde, J. L. Tate, and K. J. Schafer, Macroscopic aspects of attosecond pulse generation, J. Phys. B **41**, 132001 (2008).

[41] V. Tosa, H. T. Kim, I. J. Kim, and C. H. Nam, High-order harmonic generation by chirped and self-guided femtosecond laser pulses. I. Spatial and spectral analysis, Phys. Rev. A **71**, 063807 (2005).

[42] E. Priori *et al.*, Nonadiabatic three-dimensional model of high-order harmonic generation in the few-optical-cycle regime, Phys. Rev. A **61**, 063801 (2000).

[43] T. Brabec and F. Krausz, Intense few-cycle laser fields: Frontiers of nonlinear optics, Rev. Mod. Phys. **72**, 545 (2000).

[44] I. P. Christov, H. C. Kapteyn, and M. M. Murnane, Quasi-phase matching of high-harmonics and attosecond pulses in modulated waveguides, Opt. Express **7**, 362 (2000).

[45] C. Jin, A. T. Le, and C. D. Lin, Medium propagation effects in high-order harmonic generation of Ar and N_2, Phys. Rev. A **83**, 023411 (2011).

[46] A. T. Le, R. R. Lucchese, S. Tonzani, T. Morishita, and C. D. Lin, Quantitative rescattering theory for high-order harmonic generation from molecules, Phys. Rev. A **80**, 013401 (2009).

[47] T. Morishita, A. T. Le, Z. Chen, and C. D. Lin, Accurate Retrieval of Structural Information from Laser-Induced Photoelectron and High-Order Harmonic Spectra by Few-Cycle Laser Pulses, Phys. Rev. Lett. **100**, 013903 (2008).

[48] C. D. Lin, A. T. Le, Z. Chen, T. Morishita, and R. R. Lucchese, Strong-field rescattering physics self-imaging of a molecule by its own electrons, J. Phys. B **43**, 122001 (2010).

[49] I. P. Christov, Enhanced generation of attosecond pulses in dispersion-controlled hollow-core fiber, Phys. Rev. A **60**, 3244 (1999).

[50] C. T. Chantler, K. Olsen, R. A. Dragoset, J. Chang, A. R. Kishore, S. A. Kotochigova, and D. S. Zucker, *X-Ray Form Factor, Attenuation and Scattering Tables* (National Institute of Standards and Technology, Gaithersburg, MD, 2005).

[51] B. L. Henke, E. M. Gullikson, and J. C. Davis, X-ray interactions: Photoabsorption, scattering, transmission, and reflection at $E = 50$–$30,000$ eV, $Z = 1$–92, At. Data Nucl. Data Tables **54**, 181 (1993).

[52] N. H. Shon, A. Suda, Y. Tamaki, and K. Midorikawa, High-order harmonic and attosecond pulse generations: Bulk media versus hollow waveguides, Phys. Rev. A **63**, 063806 (2001).

[53] G. Tempea and T. Brabec, Theory of self-focusing in a hollow waveguide, Opt. Lett. **23**, 762 (1998).

[54] M. Nurhuda, A. Suda, K. Midorikawa, M. Hatayama, and K. Nagasaka, Propagation dynamics of femtosecond laser pulses in a hollow fiber filled with argon: Constant gas pressure versus differential gas pressure, J. Opt. Soc. Am. B **20**, 2002 (2003).

[55] X. Zhang, Z. Sun, Y. Wang, G. Chen, Z. Wang, R. Li, Z. Zeng, and Z. Xu, High-order harmonic and attosecond pulse generation for a few-cycle laser pulse in modulated hollow fibres, J. Phys. B **40**, 2917 (2007).

[56] E. A. J. Marcatili and R. A. Schmeltzer, Hollow metallic and dielectric waveguides for long distance optical transmission and lasers, Bell Syst. Tech. J. **43**, 1783 (1964).

[57] M. Lewenstein, P. Salières, and A. L'Huillier, Phase of the atomic polarization in high-order harmonic generation, Phys. Rev. A **52**, 4747 (1995).

[58] M. B. Gaarde, F. Salin, E. Constant, Ph. Balcou, K. J. Schafer, K. C. Kulander, and A. L'Huillier, Spatiotemporal separation of high harmonic radiation into two quantum path components, Phys. Rev. A **59**, 1367 (1999).

[59] A.-T. Le, H. Wei, C. Jin, V. N. Tuoc, T. Morishita, and C. D. Lin, Universality of Returning Electron Wave Packet in High-Order Harmonic Generation with Midinfrared Laser Pulses, Phys. Rev. Lett. **113**, 033001 (2014).

[60] M. V. Ammosov, N. B. Delone, and V. P. Krainov, Tunnel ionization of complex atoms and of atomic ions in an alternating electromagnetic field, Sov. Phys. JETP **64**, 1191 (1986).

[61] X. M. Tong and C. D. Lin, Empirical formula for static field ionization rates of atoms and molecules by lasers in the barrier-suppression regime, J. Phys. B **38**, 2593 (2005).

[62] M.-C. Chen *et al.*, Generation of bright isolated attosecond soft x-ray pulses driven by multicycle midinfrared lasers, Proc. Natl. Acad. Sci. U.S.A. **111**, E2361 (2014).

[63] H. S. Chan, Z.-M. Hsieh, W.-H. Liang, A. H. Kung, C.-K. Lee, C.-J. Lai, R.-P. Pan, and L.-H. Peng, Synthesis and measurement of ultrafast waveforms from five discrete optical harmonics, Science **331**, 1165 (2011).

[64] M. Krebs, S. Hädrich, S. Demmler, J. Rothhardt, A. Zaïr, L. Chipperfield, J. Limpert, and A. Tünnermann, Towards isolated attosecond pulses at megahertz repetition rates, Nat. Photonics **7**, 555 (2013).